Seniority $v = 5$ states in $^{89}_{41}Nb_{48}$

A. Bödeker, K. P. Lieb, C. J. Gross,* M. K. Kabadiyski, D. Rudolph, and M. Weiszflog
II. Physikalisches Institut, Universität Göttingen, D-3400 Göttingen, Federal Republic of Germany

J. Eberth
Institut für Kernphysik der Universität zu Köln, D-5000 Köln 41, Federal Republic of Germany

H. Grawe, J. Heese, and K.-H. Maier
Hahn-Meitner-Institut GmbH, D-1000 Berlin 39, Federal Republic of Germany
(Received 19 May 1993)

Yrast and yrare states in the nucleus ^{89}Nb have been studied in the reaction ^{58}Ni(^{36}Ar,5p) by measuring $\gamma\gamma$ coincidences and directional correlation orientation ratios with the OSIRIS array. In addition, γ-ray singles angular distributions have been taken with the reaction ^{58}Ni(^{35}Cl,4p). Up to the highest spins observed ($37/2^+, 33/2^-$), the states identified line up with the ones predicted by the spherical shell model, taking into account three proton particles and two neutron holes in the $g_{9/2}$ and $p_{1/2}$ single-particle orbits. The shell model also reproduces most of the measured branching and $E2/M1$ mixing ratios. The mean lifetime of the 2152 keV $17/2^-$ yrast state was determined as 0.74(7) ns.

PACS number(s): 27.50.+e, 21.10.Tg, 21.60.Cs, 21.10.Hw

Recent in-beam heavy-ion studies on the light Nb, Mo, and Tc isotopes [1–10] have given evidence for many near-spherical nuclei in the mass 80–90 region. With respect to the $Z = 38$, $N = 50$ (sub)shell closures, the large number of protons and neutron holes in the $g_{9/2}$ orbit provides the possibility of angular momentum aligned multiparticle states of high spins, without the need of collective rotation. In fact, quadrupole deformation has been found to set in below the neutron number $N = 46$ [11–13] for which nuclei the calculations of Möller and Nix [14] predict both prolate and/or oblate shapes. In our extensive studies of ^{90}Mo and ^{91}Tc [5, 10], which are $N = 48$ isotones of the nucleus ^{89}Nb to be discussed here, and of the $N = 46,47$ nuclei ^{87}Nb, ^{88,89}Mo, and ^{90}Tc, we have established the positive-parity yrast states up to or even beyond the highest angular momenta which can be reached by spin aligning the $g_{9/2}$ particles holes. The negative-parity sequences have been explained by considering one valence nucleon hole in the $p_{1/2}$ orbit. The predicted wave functions follow a rather simple seniority scheme, with a predominant component of some 50% belonging to a single configuration and typically 80% to a definite seniority.

According to this scheme, high-spin states in ^{89}Nb can be grouped into seniority $v = 3$ states reaching up to spin $25/2^+$ and $19/2^-$, having either two neutron holes and one proton or three protons. The seniority $v = 5$ states having two neutron holes and three protons then should extend up to spins $37/2^+$ and $33/2^-$. The yrast states of the $v = 3$ group, including the 2193 keV $21/2^+$ isomer ($\tau = 21$ ns), have been identified via light-ion-induced reactions [15–17] and the electron capture (EC) β^+ decay of ^{89}Mo [18], but very little information is available for the $v = 5$ levels. According to the shell model calculations of ^{89}Nb (see below) and results in the isobar ^{89}Mo [4], these states should be at 3–7 MeV excitation and some of their decays characterized by strong $M1$ transitions [4, 19]. It was the aim of the present study to search for these states and to determine and explain their decay properties.

High-spin states in ^{89}Nb were populated with the reaction ^{58}Ni(^{36}Ar,5p) by using the 149 MeV ^{36}Ar beam of the VICKSI accelerator in Berlin and a 19.8 mg/cm^2 metallic ^{58}Ni foil isotopically enriched to 99.98%. The γ radiation was measured in the OSIRIS array, consisting of 12 Compton-suppressed Ge detectors positioned at 65° and 115° symmetrically around the beam axis. Another large-volume Ge detector was placed at 162° to the beam. Evaporated neutrons, protons, and α particles were measured in several NE213 and Δ-E surface barrier detectors. Details of the experimental setup, data accumulation, and analysis have been communicated in previous papers [3, 5]. As the lower part of the ^{89}Nb yrast spectrum was known [15–18], no identification of the residual nucleus was required and the level scheme was established by means of standard $\gamma\gamma$ spectroscopy. It was, however, verified that the new γ-ray lines in ^{89}Nb have the correct intensity ratios in the particle-gated γ-coincidence matrices, typical for zero neutron and α-particle multiplicity and fivefold proton multiplicity (for details see [3, 4, 7]). In addition, directional correlation orientation (DCO) ratios were measured between the 162° detector and the

*Present address: Oak Ridge National Laboratory, Oak Ridge, TN 37831.

two OSIRIS rings by evaluating the intensity ratios:

$$R_{\mathrm{DCO}} = \frac{Y(E_1 \text{ at } 162^\circ;\ E_2 \text{ recorded in rings})}{Y(E_1 \text{ in rings};\ E_2 \text{ recorded at } 162^\circ)} .$$

The coincidence intensities $Y(E_1,E_2)$ were efficiency corrected with respect to all detectors involved [5, 20]. The DCO ratios were calibrated with respect to previously known $E2$ and $E1$ transitions in residual nuclei populated in the same ^{58}Ni + ^{36}Ar experiment [2–5, 7]. In all cases, stretched $E2$ gating transitions were used. The detailed formulas appropriate for evaluating the angular correlations for this detector geometry are given in a recent paper by Kabadiyski *et al.* [20]. In a separate recoil distance lifetime measurement of the same reaction, we determined the mean lifetime of the 2152 keV $17/2^-$ state to be $\tau = 0.74(7)$ ns. This value is in agreement with the upper limit $\tau < 6$ ns measured by Spalek *et al.* [17], but at variance with the result of an electronic timing experiment, $\tau = 9(6)$ ns [15].

TABLE I. Level energies and γ-ray energies, intensities, angular distributions and DCO ratios in ^{89}Nb.

E_x (keV)	E_γ (keV)	Intensity[a]	R_{DCO}[b]	A_2	A_4	$I_i^\pi \rightarrow I_f^\pi$[d]
659.0(2)	659.0(2)	—				$(7/2^+)\rightarrow 9/2^+$
1003.4(1)	1003.4(1)	111(3)[c]	0.94(8)^B			$13/2^+\rightarrow 9/2^+$
1935.3(1)	931.8(1)	100(3)[c]	0.98(8)^A			$17/2^+\rightarrow 13/2^+$
2151.5(1)	216.2(1)	32(3)	0.86(8)^A	0.35(4)	0.08(4)	$17/2^-\rightarrow 17/2^+$
2191.5(2)	1188.1(2)	10.9(5)				$\rightarrow 13/2^+$
2192.9(1)	257.7(1)	63(3)[c]				$21/2^+\rightarrow 17/2^+$
2518.2(1)	366.7(2)	3.7(5)				$\rightarrow 17/2^-$
2523.0(1)	330.1(1)	4.6(11)				$(19/2^+)\rightarrow 21/2^+$
2955.7(1)	762.8(1)	50(3)	0.57(7)^C	-0.27(2)	0.05(2)	$23/2^+\rightarrow 21/2^+$
3141.9(2)	990.3(1)	20.8(22)	1.10(11)^A	0.28(2)	-0.02(2)	$21/2^-\rightarrow 17/2^-$
	619.0(1)	3.6(5)				$\rightarrow 19/2^+$
	949.0(2)	0.3(1)				$\rightarrow 21/2^+$
3403.0(2)	447.3(1)	39(4)	0.57(7)^C	-0.46(3)	0.08(3)	$25/2^+\rightarrow 25/2^+$
3805.7(2)	663.7(1)	21.3(26)	1.05(12)^D	0.30(2)	0.01(7)	$25/2^-\rightarrow 21/2^-$
	402.7(1)	15.8(16)		0.39(3)	0.01(3)	$\rightarrow 25/2^+$
	850.1(2)	1.2(2)				$\rightarrow 23/2^+$
4076.0(2)	1883.1(2)	5.8(6)		0.17(2)	-0.02(3)	$25/2^+\rightarrow 21/2^+$
	1120.3(1)	3.7(4)		-0.39(3)	0.01(3)	$\rightarrow 23/2^+$
4553.6(2)	747.9(1)	20.8(22)	0.51(8)^D	-0.44(3)	0.05(4)	$27/2^-\rightarrow 25/2^-$
4797.2(3)	721.2(2)	2.0(5)				$\rightarrow 25/2^+$
4808.7(3)	255.1(1)	15.1(20)	0.52(9)^D	-0.39(2)	0.02(2)	$29/2^-\rightarrow 27/2^-$
	1003.0(1)	9.5(29)				$\rightarrow 25/2^-$
4908.5(2)	354.8(2)	1.9(4)				$\rightarrow 27/2^-$
5041.3(2)	1638.3(2)	15.2(15)	0.98(20)^E	0.30(2)	-0.03(2)	$29/2^+\rightarrow 25/2^+$
	965.3(1)	4.0(8)				$\rightarrow 25/2^+$
	244.2(2)	1.6(3)				
5324.2(3)	515.4(1)	8.6(10)	0.65(22)^D			$(31/2^-)\rightarrow 29/2^-$
5407.3(3)	1601.6(2)	3.9(5)				$\rightarrow 25/2^-$
	853.8(2)	2.1(2)				$\rightarrow 27/2^-$
	498.4(3)	1.3(2)				
5697.8(3)	373.6(1)	4.8(7)	0.53(16)^D			$(33/2^-)\rightarrow (31/2^-)$
5917.0(3)	875.7(3)	1.1(2)				$\rightarrow 29/2^+$
6100.2(3)	1058.8(1)	12.0(12)	1.09(17)^C	0.34(3)	0.01(5)	$33/2^+\rightarrow 29/2^+$
	402.5(2)	3.4(17)	0.95(19)^D			$\rightarrow (33/2^-)$
	183.2(3)	1.2(2)				
6131.5(3)	724.3(2)	7.2(10)				
6451.8(3)	320.3(1)	3.9(6)				
6547.4(3)	1738.9(2)	2.9(4)				
	1223.2(2)	1.3(2)				
	416.0(2)	3.0(5)				
6658.3(3)	558.1(2)	2.8(5)				
6949.6(3)	497.8(2)	3.2(4)				
7271.6(6)	614.3(5)	2.1(4)				

[a] γ-ray intensity at 65°.

[b] Gates set on transitions of A, 1003 keV; B, 932 keV, C, 1638 keV; D, 990 keV; E, 1059 keV.

[c] No angular distributions evaluated for transitions in the cascade depopulating the isomeric state, because of hyperfine deorientation in the ^{58}Ni target.

[d] No spin-parity assignments included from shell model calculations.

In order to check the spin-parity assignments and γ-ray multipolarities proposed on the basis of the DCO ratios, we also performed angular-distribution measurements of the reaction ^{58}Ni(^{35}Cl,4p)^{89}Nb at 120 MeV beam energy, using the Köln tandem accelerator. Both experiments provided the γ-ray energies and intensities, DCO ratios, angular-distribution coefficients, level energies, and spin-parity assignments listed in Table I and the level scheme displayed in Fig. 1. The present experiment confirms the levels up to the previously identified 3403 keV $25/2^+$ and 4554 keV $(27/2)^-$ states [15–18], with one exception: the 258 keV line was found to be a doublet with a second component of 255 keV.

The positive-parity yrast line starts with the $9/2^+$ ground state and was extended up to the 7272 keV level which most probably has spin and parity $37/2^+$. On top of the 2193 keV $21/2^+$ isomer, we located several stretched $E2$ and $M1$ transitions, involving the 3403 keV $25/2^+$, 5041 keV $29/2^+$, and 6100 keV $33/2^+$ yrast states and the 4076 keV $25/2_2^+$ yrare state. Three new levels above 4.5 MeV are indicated as tentative as the intensity balance of feeding and depopulating transitions did not allow unambiguous placements. The negative-parity yrast sequence extends up to the 5698 keV level which most probably has $33/2^-$. An additional sequence of states at 4909, 5407, 6132, 6452, 6547, and 6950 keV excitation is very weakly populated; for that reason, neither DCO ratios nor angular-distribution coefficients could be evaluated and, hence, no spins are given. We also identified a number of transitions between the negative- and positive-parity levels. Among them, the only transition for which the DCO ratio could be determined is the 216 keV $17/2^- \rightarrow 17/2^+$ γ ray whose quadrupole/dipole mixing ratio is indeed consistent with zero as expected for a parity-changing transition. The 403 keV line turned out to be a doublet of two ΔI=0 parity-changing transitions: $33/2^+ \rightarrow (33/2)^-$ and $25/2^- \rightarrow 25/2^+$. Evidence for the doublet structure comes from the relative intensities of the 403 keV and 447 keV transitions when gating on the upper 255 keV line, from the observation of the 558 keV and 614 keV lines in this gate and from the fact that the 403 keV line is coincident with itself.

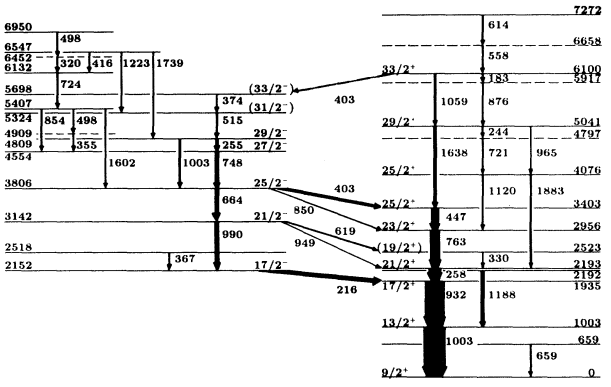

FIG. 1. Observed high-spin level scheme of ^{89}Nb. The dashed level energies indicate that the order of the feeding and depopulating transitions could not be resolved on the basis of the γ-ray intensities.

Earlier work on the $N = 49$ and $N = 50$ isotones above $Z = 38$ has shown that their structures are well described by the spherical shell model using a ^{88}Sr core [16, 21–24]. In view of the success of similar calculations for a number of $N = 46$–48 nuclei up to the highest spins observed, in particular for the $N = 48$ isotones ^{88}Zr and ^{90}Tc [8, 9], we have calculated the yrast spectrum in ^{89}Nb by means of the Utrecht shell model code RITSSCHIL [25]. As in most of our previous papers we have restricted the model space to the $g_{9/2}$ and $p_{1/2}$ single-particle orbits outside the semimagic ^{88}Sr core. Core excitations of vibrational type, as for instance included in the interpretation of ^{86}Zr in the frame of the interacting boson model [19], and other orbits in the $1f2p$ and $3s2d$ shells have been neglected. Oxorn *et al.* [16] have pointed out that the low-spin states in ^{89}Nb up to $13/2^+$ contain complex core-coupled components. The single-particle energies and effective two-body matrix elements are those deduced by Gross and Frenkel [23]. The calculated level energies are indicated in Fig. 2 and, indeed, compare very well with the measured states. Note that the theoretical level scheme has been shifted by 153 keV in order to adjust the experimental and theoretical $21/2^+$ yrast states. The mean energy deviation of all yrast states above spin $17/2^-$ and $25/2^+$ and the $25/2^+$ and $17/2^-$

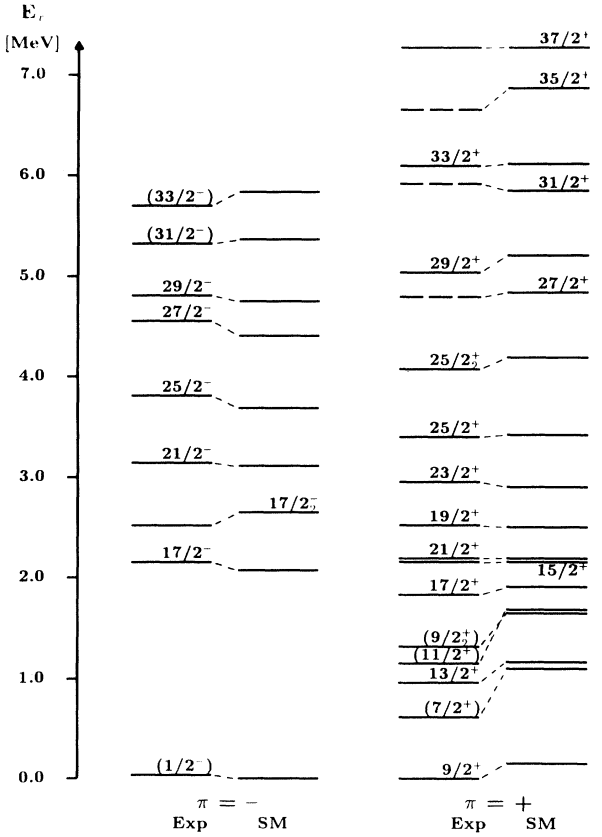

FIG. 2. Experimental and calculated high-spin states in ^{89}Nb. Experimental spin-parity assignments are indicated at the experimental levels, those inferred from the shell model calculations at the theoretical levels.

yrare states is 114 keV. Considering the levels above 4.5 MeV excitation for which no experimental spin-parity assignments could be made, it is tempting to associate the calculated $27/2^+$, $31/2^+$, $35/2^+$, and $37/2^+$ yrast states with the observed levels at 4797, 5917, 6658, and 7272 keV, as indicated in Fig. 2. The angular momenta of the five valence nucleons can thereby couple to the seniority $v = 5$ configurations $[\pi^3(g_{9/2}) \otimes \nu^{-2}(g_{9/2})]_{I \leq 37/2}$ and $[\pi^2(g_{9/2}) \otimes \pi(p_{1/2}) \otimes \nu^{-2}(g_{9/2})]_{I \leq 33/2}$. So far no $19/2^-$ levels have been identified experimentally. The calculation predicts the $19/2^-$ yrast state at 3.194 MeV to have predominantly a $v = 5$ configuration, while the fully stretched $[\pi(g_{9/2}) \otimes \pi(p_{1/2}) \otimes \nu^{-1}(g_{9/2})]$ $v = 3$ state should lie at 3.312 MeV.

When inspecting the calculated wave functions, the states above $I^\pi = 25/2^+$ and $19/2^-$ must have seniority $v = 5$, within the truncated model space used. The question arises as to what spins and seniorities the proton particles and neutron holes couple individually and to what extent the predicted wave functions reproduce the measured γ-ray decay properties. Table II summarizes the main components of the wave functions, while Table III lists the calculated and experimental branching and $E2/M1$ mixing ratios. We used the calculated transition energies and the slightly quenched single-particle magnetic moments $g_l^\pi = 0.97$, $g_s^\pi = 4.70$, $g_l^\nu = 0.13$, $g_s^\nu = -3.24$ which reproduce the magnetic moments of the $9/2^+$ and $1/2^-$ states in ^{87}Sr and ^{89}Y and the 8^+ states in ^{90}Zr-^{96}Pd. The effective proton charge used, $e_{\rm eff}^\pi = e + \delta e^\pi = 1.72e$, is that deduced in [18], giving the estimate $e_{\rm eff}^\nu \approx 2\delta e^\pi = 1.44e$ [26]. These large effective charges are, of course, a consequence of the very much restricted single-particle space. The calculations reproduce the small $E2/M1$ mixing ratios of all stretched $\Delta I = -1$ transitions and most of the branching ratios (see Table III). The small mixing ratios document the absence of collective degrees of freedom and the possibility of spin recouplings within similar configurations having identical proton and neutron seniorities. Consequently, most calculated lifetimes of states above spin $21/2^+$ are in the 0.1–1.5 ps range, i.e., rather short. Concerning the branching ratios, the changes between strong stretched $\Delta I = -2$ and $\Delta I = -1$ transitions along the yrast lines of both parities are well accounted for. A prominent ex-

TABLE II. Predicted major components of the shell-model wave functions of high-spin states in ^{89}Nb. Only components with more than 20% are given.

I^π	v	Partition[a]	Component (%)	I^π	v	Partition[a]	Component (%)
$9/2^+$	1	π	86	$17/2^-$	3	$(\pi'\pi_8^2)_{17/2}$	77
$13/2^+$	3	$\pi \otimes \nu_2^{-2}$	83	$17/2_2^-$	3	$\pi \otimes (\nu'^1\nu^{-1})_5$	36
$15/2^+$	3	$\pi \otimes \nu_6^{-2}$	49		3	$\pi' \otimes \nu_8^{-2}$	22
	3	$\pi \otimes \nu_4^{-2}$	38	$19/2^-$[b]	5	$(\pi'\pi_2^2)_{3/2} \otimes \nu_8^{-2}$	34
$17/2^+$	3	$\pi \otimes \nu_4^{-2}$	68	$19/2_2^-$[c]	3	$\pi \otimes (\nu'\nu^{-1})_5$	89
	3	$\pi \otimes \nu_6^{-2}$	20	$21/2^-$	5	$(\pi'\pi_8^2)_{17/2} \otimes \nu_2^{-2}$	73
$19/2^+$	3	$\pi \otimes \nu_8^{-2}$	71	$23/2^-$[d]	5	$(\pi'\pi_8^2)_{17/2} \otimes \nu_8^{-2}$	25
	5	$\pi_{9/2}^3 \otimes \nu_8^{-2}$	22	$25/2^-$	5	$(\pi'\pi_8^2)_{17/2} \otimes \nu_4^{-2}$	26
$21/2^+$	3	$\pi \otimes \nu_8^{-2}$	64		5	$(\pi'\pi_8^2)_{17/2} \otimes \nu_8^{-2}$	20
	3	$\pi \otimes \nu_6^{-2}$	28	$27/2^-$	5	$(\pi'\pi_8^2)_{17/2} \otimes \nu_8^{-2}$	70
$23/2^+$	3	$\pi \otimes \nu_8^{-2}$	93	$29/2^-$	5	$(\pi'\pi_8^2)_{17/2} \otimes \nu_6^{-2}$	54
$25/2^+$	3	$\pi \otimes \nu_8^{-2}$	95		5	$(\pi'\pi_6^2)_{13/2} \otimes \nu_8^{-2}$	44
$25/2_2^+$	5	mixed		$31/2^-$	5	$(\pi'\pi_8^2)_{17/2} \otimes \nu_8^{-2}$	99
$27/2^+$	5	$\pi_{13/2}^3 \otimes \nu_8^{-2}$	51	$33/2^-$	5	$(\pi'\pi_8^2)_{17/2} \otimes \nu_8^{-2}$	100
	5	$\pi_{11/2}^3 \otimes \nu_8^{-2}$	31				
$29/2^+$	5	$\pi_{13/2}^3 \otimes \nu_8^{-2}$	53				
	5	$\pi_{17/2}^3 \otimes \nu_6^{-2}$	25				
$31/2^+$	5	$\pi_{15/2}^3 \otimes \nu_8^{-2}$	43				
	5	$\pi_{17/2}^3 \otimes \nu_8^{-2}$	38				
$33/2^+$	5	$\pi_{17/2}^3 \otimes \nu_8^{-2}$	52				
	5	$\pi_{21/2}^3 \otimes \nu_8^{-2}$	29				
	5	$\pi_{21/2}^3 \otimes \nu_6^{-2}$	20				
$35/2^+$	5	$\pi_{21/2}^3 \otimes \nu_8^{-2}$	100				
$37/2^+$	5	$\pi_{21/2}^3 \otimes \nu_8^{-2}$	100				

[a] Nomenclature: $\pi = \pi(g_{9/2})$, $\pi' = \pi(p_{1/2})$, $\nu = \nu(g_{9/2})$, $\nu' = \nu(p_{1/2})$, $(\pi'\pi^2)_{Ip} \otimes \nu_{In}^{-2}$, $I_p + I_n = I$.

[b] Calculated energy $E(19/2_1^-)$=3.194 MeV.

[c] Calculated energy $E(19/2_2^-)$=3.312 MeV.

[d] Calculated energy $E(23/2_2^-)$=3.597 MeV.

ample is the $25/2^+ \rightarrow 23/2^+ \rightarrow 21/2^+$ cascade within the $v = 3$ configurations: The $25/2^+$ state is predicted to have a 95% fully aligned $[\pi(g_{9/2}) \otimes \nu^{-2}(g_{9/2})_8]$ partition, while the $23/2^+$ and $21/2^+$ states should still have 93% and 64% components of this partition, respectively. This leads to large $M1$ strengths, i.e., $B(M1, 25/2^+ \rightarrow 23/2^+) = 1.7\mu_N^2$, and small $E2$ strengths. The expected small $25/2^+ \rightarrow 21/2^+$ branch of 2% has not been observed, indeed. This is a further argument in favor of the spin-parity assignments proposed in Fig. 2. Likewise, the exclusive decay of the 2518 keV state to the 2152 keV $17/2^-$ state and the absence of a $3142 \rightarrow 2518$ keV branch suggest the 2518 keV level to be the $17/2^-$ yrare state. However, there are two noteworthy exceptions: the decays of the 4809 keV $29/2^-$ and the 6100 keV $33/2^+$ states are not reproduced by the shell model calculations. In the case of the 4809 keV $29/2^-$ state, this discrepancy can be traced to the very small predicted $29/2^- \rightarrow 27/2^-$ transition strengths of $B(E2) = 0.87\ e^2\,\mathrm{fm}^4$ and $B(M1) = 0.11\mu_N^2$ which are by 1 to 2 orders of magnitude smaller than the usual strengths, probably due to an accidental cancellation. Also the $33/2^+$ state appears to have a more complex wave function with several large components (see Table III).

A further check on the reliability of the shell model description is the 21(4) ns mean lifetime of the isomeric $21/2^+$ state at 2193 keV [15, 17]. If we insert the experimental decay energy of 258 keV, we arrive at an expected lifetime of 13 ns. This is somewhat smaller than the experimental value and may indicate that the effective $E2$ neutron charge for the higher-spin states is slightly smaller. Diana *et al.* [15] have suggested that

TABLE III. Experimental and theoretical branching (B) and mixing ratios $\delta(E2/M1)$ of transitions in ^{89}Nb (branching ratios and $E2/M1$ mixing ratios calculated with theoretical transition energies).

E_x (keV)	E_γ (keV)	$I_i^\pi \rightarrow I_f^\pi$	B (%) Expt.	B (%) Theor.	$\delta(E2/M1)$ Expt.[a]	$\delta(E2/M1)$ Theor.
7272	614	$(37/2^+) \rightarrow (35/2^+)$	100	93		0.02
	1173	$\rightarrow 33/2^+$	n.o[c]	7		
6658	558	$(35/2^+) \rightarrow 33/2^+$	100	99		0.04
	741	$\rightarrow (31/2^+)$	n.o.	1		
6100	1059	$33/2^+ \rightarrow 29/2^+$	73(8)[b]	19		
	183	$\rightarrow (31/2^+)$	6(2)[b]	81		0.02
5917	876	$(31/2^+) \rightarrow 29/2^+$	100	67		0.05
	1120	$\rightarrow (27/2^+)$	n.o.	33		
5041	1638	$29/2^+ \rightarrow 25/2^+$	74(6)	54		
	244	$\rightarrow 27/2^+$	19(5)	40		0.03
	965	$\rightarrow 25/2_2^+$	7(2)	6		
4797	721	$(27/2^+) \rightarrow 25/2_2^+$	100	81		0.04
	1841	$\rightarrow 23/2^+$	n.o.	18		
4076	1883	$25/2_2^+ \rightarrow 21/2^+$	66(5)	61		
	1120	$\rightarrow 23/2^+$	34(5)	34	0.12(7)	0.05
	673	$\rightarrow 25/2^+$	n.o.	4		0.05
3403	447	$25/2^+ \rightarrow 23/2^+$	100	98	0.10(5)	0.04
	1210	$\rightarrow 21/2^+$	n.o.	2		
2956	763	$23/2^+ \rightarrow 21/2^+$	100	100	0.03(2)	0.05
2523	330	$(19/2^+) \rightarrow 21/2^+$	100	99		0.02
	588	$\rightarrow 17/2^+$	n.o.	1		0.11
	331	$\rightarrow 15/2^+$	n.o.	0		
2192	1188	$15/2^+ \rightarrow 13/2^+$	100	73		0.28
	257	$\rightarrow 17/2^+$	n.o.	26		0.02
5698	374	$(33/2^-) \rightarrow (31/2^-)$	100	99		0.04
	889	$\rightarrow 29/2^-$	n.o.	1		
5324	515	$(31/2^-) \rightarrow 29/2^-$	100	60		0.03
	770	$\rightarrow 27/2^-$	n.o.	0		
4809	255	$29/2^- \rightarrow 27/2^-$	57(10)	5	0.09(4)	0.03
	1003	$\rightarrow 25/2^-$	43(10)	95		
4554	748	$27/2^- \rightarrow 25/2^-$	100	100	0.09(6)	0.04
3806	664	$25/2^- \rightarrow 21/2^-$	56(6)[b]	100		
3142	990	$21/2^- \rightarrow 17/2^-$	87(3)[b]	100		
	624	$\rightarrow (17/2_2^-)$	n.o.	0		
2518	367	$(17/2_2^-) \rightarrow 17/2^-$	100	100		0.05

[a] Average values of $\delta(E2/M1)$ from DCO and angular-distribution data.

[b] The remaining decay branches are via $E1$ which are forbidden in the shell model space considered.

[c] Transition not observed.

the lifetime of the $21/2^+$ isomer requires $[\pi^3(g_{9/2})]$ and $[\pi(g_{9/2}) \otimes \nu^{-2}(g_{9/2})]$ $v = 3$ components in its wave function; we find a 92% partition of the latter type.

In conclusion, the newly identified seniority $v = 5$ yrast states in ^{89}Nb follow the patterns found for the seniority $v = 3$ states in this nucleus [15, 16] and in several neighboring nuclei: the full valence space of particles and holes in the $g_{9/2}$ and $p_{1/2}$ orbits relative to ^{88}Sr is exhausted to align the individual single-particle angular momenta up to maximum spins allowed by the Pauli principle. In this fashion, $v = 5$ states up to $(37/2^+)$ and $(33/2^-)$ have been established. The overall success of the shell model with this very much restricted model space is surprising, indeed. It is important to note that no attempt was made to modify either the two-body matrix elements or the effective electromagnetic coupling constants, but we have used the parameters derived previously from the lower seniority states in this mass region. The close agreement of experimental and calculated energies at the very highest spins found in ^{89}Nb as in many other isotopes of this mass region implies that the shell model has a good predictive power, in spite of the very limited single-particle base. The effects of using a larger single-particle base have been discussed, e.g., for the high-spin spectrum of the $N = 48$ isotone ^{90}Mo [5]. It may well be that the weakly excited states feeding the $25/2^-$-$31/2^-$ yrast states in ^{89}Nb (see Fig. 1) are due to excitations from the $2p_{3/2}$ and $1f_{5/2}$ single-particle orbits.

This research was supported by Deutsches Bundesministerium für Forschung und Technologie. It is a pleasure to acknowledge the vigorous support of the accelerator crews at Berlin and Köln and the help of J. Altmann, F. Cristancho, A. Jungclaus, T. Mylaeus, and S. Skoda in part of the experiments.

[1] B.J. Min, S. Suematsu, S. Mitarai, T. Kuroyanagi, U. Heiguchi, and M. Matsuzaki, Nucl. Phys. **A530**, 211 (1991).

[2] A. Jungclaus, K.P. Lieb, C.J. Gross, J. Heese, D. Rudolph, D.J. Blumenthal, P. Chowdhury, P.J. Ennis, C.J. Lister, Ch. Winter, J. Eberth, T. Skoda, W. Gelletly, and B.J. Varley, Z. Phys. A **530**, 125 (1991).

[3] M. Weiszflog, K.P. Lieb, F. Cristancho, C.J. Gross, A. Jungclaus, D. Rudolph, H. Grawe, J. Heese, K.-H. Maier, J. Eberth, and S. Skoda, Z. Phys. A **342**, 257 (1992).

[4] M. Weiszflog, C.J. Gross, M.K. Kabadiyski, K.P. Lieb, D. Rudolph, H. Grawe, J. Heese, K.-H. Maier, J. Eberth, and S. Skoda, Z. Phys. A **344**, 395 (1993).

[5] M.K. Kabadiyski, F. Cristancho, C.J. Gross, A. Jungclaus, K.P. Lieb, D. Rudolph, H. Grawe, J. Heese, K.-H. Maier, J. Eberth, S. Skoda, W.-T. Chou, and E.K. Warburton, Z. Phys. A **343**, 165 (1992).

[6] S.E. Arnell, D. Foltescu, H.A. Roth, Ö. Skeppstedt, A. Nilsson, S. Mitarai, and J. Nyberg, Phys. Scr. **46**, 355 (1992).

[7] D. Rudolph, F. Cristancho, C.J. Gross, A. Jungclaus, K.P. Lieb, H. Grawe, J. Heese, K.-H. Maier, J. Eberth, and S. Skoda, Z. Phys. A **342**, 121 (1992).

[8] D. Rudolph, C.J. Gross, M.K. Kabadiyski, K.P. Lieb, M. Weiszflog, H. Grawe, J. Heese, K.-H. Maier, and J. Eberth, Phys. Rev. C **47**, 2574 (1993).

[9] S.E. Arnell, D. Foltescu, H.A. Roth, Ö. Skeppstedt, A. Nilsson, S. Mitarai, and J. Nyberg, Phys. Scr. **47**, 142 (1993).

[10] D. Rudolph, C.J. Gross, A. Harder, M. Kabadiyski, K.P. Lieb, M. Weiszflog, H. Grawe, J. Heese, K.-H. Maier, J. Altmann, A. Dewald, and T. Mylaeus, submitted to Phys. Rev. C.

[11] Ch. Winter, D.J. Blumenthal, P. Chowdhury, B. Crowell, P.J. Ennis, S.J. Freeman, C.J. Lister, C.J. Gross, J. Heese, A. Jungclaus, K.P. Lieb, D. Rudolph, M.A. Bentley, W. Gelletly, J. Simpson, J.L. Durell, and B.J. Varley, Nucl. Phys. **A535**, 137 (1991).

[12] C.J. Gross, K.P. Lieb, D. Rudolph, M.A. Bentley, W. Gelletly, H.G. Price, J. Simpson, D.J. Blumenthal, P. Chowdhury, P.J. Ennis, C.J. Lister, Ch. Winter, J.L. Durell, B.J. Varley, O. Skeppstedt, and S. Rastikerdar, Nucl. Phys. **A535**, 203 (1991).

[13] C.J. Gross, W. Gelletly, M.A. Bentley, H.G. Price, J. Simpson, K.P. Lieb, D. Rudolph, J.L. Durell, B.J. Varley, and S. Rastikerdar, Phys. Rev. C **44**, R2253 (1991).

[14] P. Möller and J.R. Nix, At. Data Nucl. Data Tables **26**, 165 (1981).

[15] B.J. Diana, F. W. N. de Boer, and C.A. Fields, Z. Phys. A **306**, 171 (1982).

[16] K. Oxorn, S.K. Mark, J.E. Kitching, and S.S.M. Wong, Z. Phys. A **321**, 485 (1985).

[17] A. Spalek, J. Adam, J. Jursik, A. Kuklik, L. Maly, D. Venos, P. Simecek, G. Winter, and L. Funke, Nucl. Phys. **A280**, 115 (1977).

[18] P.W. Gallagher, N.K. Arras, and W.B. Walter, Phys. Rev. C **23**, 873 (1981).

[19] P. Chowdhury, C.J. Lister, D. Vretenaer, Ch. Winter, V.P. Janzen, H.R. Andrews, D.J. Blumenthal, B. Crowell, T. Drake, P.J. Ennis, A. Galindo-Uribarri, D. Horn, J.K. Johansson, A. Omar, S. Pivotte, D. Prevost, D. Radford, J.C. Waddington, and D. Ward, Phys. Rev. Lett. **67**, 2950 (1991).

[20] M.K. Kabadiyski, K.P. Lieb, and D. Rudolph, Nucl. Phys. A (in press).

[21] D.H. Gloeckner, and F.J.D. Serduke, Nucl. Phys. **A220**, 477 (1974).

[22] F.J.D. Serduke, R.D. Lawson, and D.H. Gloeckner, Nucl. Phys. **A256**, 45 (1976).

[23] R. Gross and A. Frenkel, Nucl. Phys. **A267**, 85 (1976).

[24] A. Amusa and R.D. Lawson, Z. Phys. A **314**, 205 (1983).

[25] D. Zwarts, code RITSSCHIL, Comput. Phys. Commun. **38**, 365 (1985).

[26] P. Raghavan, M. Senba, Z.Z. Ding, A. Lopez-Garcia, B.A. Brown, and R.S. Raghavan, Phys. Rev. Lett. **54**, 2592 (1985).